Efficient and robust ventricular tachycardia and fibrillation detection method for wearable cardiac health monitoring devices

Eedara Prabhakararao ✉, *M. Sabarimalai Manikandan*

School of Electrical Sciences, Indian Institute of Technology Bhubaneswar, Bhubaneswar, Odisha 751013, India
✉ *E-mail: pe10@iitbbs.ac.in*

Published in Healthcare Technology Letters; Received on 8th March 2016; Revised on 15th June 2016; Accepted on 16th June 2016

In this Letter, the authors propose an efficient and robust method for automatically determining the VT and VF events in the electrocardiogram (ECG) signal. The proposed method consists of: (i) discrete cosine transform (DCT)-based noise suppression; (ii) addition of bipolar sequence of amplitudes with alternating polarity; (iii) zero-crossing rate (ZCR) estimation-based VTVF detection; and (iv) peak-to-peak interval (PPI) feature based VT/VF discrimination. The proposed method is evaluated using 18,000 episodes of different ECG arrhythmias taken from 6 PhysioNet databases. The method achieves an average sensitivity (Se) of 99.61%, specificity (Sp) of 99.96%, and overall accuracy (OA) of 99.92% in detecting VTVF and non-VTVF episodes by using a ZCR feature. Results show that the method achieves a Se of 100%, Sp of 99.70% and OA of 99.85% for discriminating VT from VF episodes using PPI features extracted from the processed signal. The robustness of the method is tested using different kinds of ECG beats and various types of noises including the baseline wanders, powerline interference and muscle artefacts. Results demonstrate that the proposed method with the ZCR, PPI features can achieve significantly better detection rates as compared with the existing methods.

1. Introduction: Life-threatening arrhythmias such as ventricular fibrillation (VF) and rapid ventricular tachycardia (VT) are dangerous arrhythmic events leading to sudden cardiac death (SCD) problems [1–21]. If VT persists for a certain period of time, it may induce VF event, which is the main cause of SCD problems. Therefore, early detection of VT/VF events is most essential for an automatic external defibrillator (AED) which can timely deliver an electric shock therapy, and remote monitoring of cardiac patients by means of simple, robust and accurate automated methods.

Numerous VT/VF detection methods have been proposed based on the combination of signal processing and machine learning techniques such as morphological and spectral parameters [3], autocorrelation function [4], time-delay methods [8], threshold-crossing sample counts (TCSC) [9], threshold-crossing intervals (TCls) [10], sequential hypothesis testing algorithm [10], mean signal strength and empirical mode decomposition (EMD) functions [11], leakage/complexity measure [12], dynamic sample entropy [13], non-linear prediction [17], band-pass filter and electrocardiogram (ECG) peak detection [18], multifractal singularity spectrum [19], wavelet transforms (WTs) [6, 20] and the machine learning techniques such as neural networks [2, 22], support vector machines (SVMs) [3] and fuzzy neural networks [19]. Some methods use the feature selection (FS) techniques such as genetic algorithm (GA) [5], linear discriminant analysis (LDA) [6], and non-overlap area distribution measurement (NADM) [23].

In [2], a VT/VF classification method is presented using the total of 14 metrics extracted from 5 s ECG signal, GA-based FS and the SVM classifier. A method for detection of life-threatening events is reported based on the total of 13 parameters including temporal (morphological), spectral, and complexity features of the ECG signal, combination of filter-type FS procedures, and the SVM classifier [3]. The performance of combining previously defined 11 ECG parameters such as TCI, standard exponential, modified exponential, complexity measurement, VF filter (VFleak), spectral algorithm (M and A2 parameters), median frequency, mean absolute value (MAV), phase space reconstruction (PSR) and Hilbert transform (HT) for the detection of life-threatening arrhythmias using the SVM classifier [5]. Results showed that the VFleak, HT, and PSR features result in best detection rates. A wavelet based method is presented to discriminate the ventricular arrhythmias using the number of islands, average time-width features extracted from the scalogram and LDA classifier [6]. A life threatening arrhythmia detection algorithm using the 14 features extracted from the detail coefficients at levels of 3 and 4 of the Haar transform [7]. The optimal features were selected using NADM based on the neural fuzzy network. A time-delay methods is proposed for detecting VF events using the mean subtraction, moving averaging filter, drift suppression and Butterworth filter with a cut-off frequency of 30 Hz eliminates frequencies higher than 30 Hz [8]. The detection performance of four techniques such as TCI, peaks in the ACF, VF-filter, and signal spectrum shape is studied using 4 s long 70 segments and 40 segments from the VF and VF-like recordings, respectively [15]. The TCI algorithm had a sensitivity (Se) of 93% and specificity (Sp) of 60%. The spectrum, VF filter, and ACF algorithms had overall sensitivity values of 80, 93, and 87%, and overall specificity values of 60, 20, and 0%, respectively. In [17], a reduction of the sensitivity and specificity was studied under noisy environments. Results showed that the TCSC and MAV features may not result in better detection rates under different ECG noises and time-varying PQRST morphologies with tall P- and T-waves, and wide QRS complexes. A real-time ventricular arrhythmias algorithm is presented based on the Karhunen–Loev transform and sequential-hypothesis testing and a total of four parameters including average to peak ratio, TCI, duty cycle, and delta zero-crossing interval [21]. In our previous work, detection of life-threatening arrhythmias is studied using random noise and zero crossing information [24]. The limitations of the existing methods are summarised as follows:

(i) Computationally expensive signal decomposition techniques such as WT, EMD are used for characterising the ECG waveform from the noise and artefacts, and extracting the representative features.
(ii) Most methods use sets of ECG features to discriminate non-VTVF from VTVF events and detect of VT/VF events.
(iii) Machine learning-based VT/VF detection methods highly demand a large collection of all possible ECG beats and VT/VF events to find the optimal model parameters.

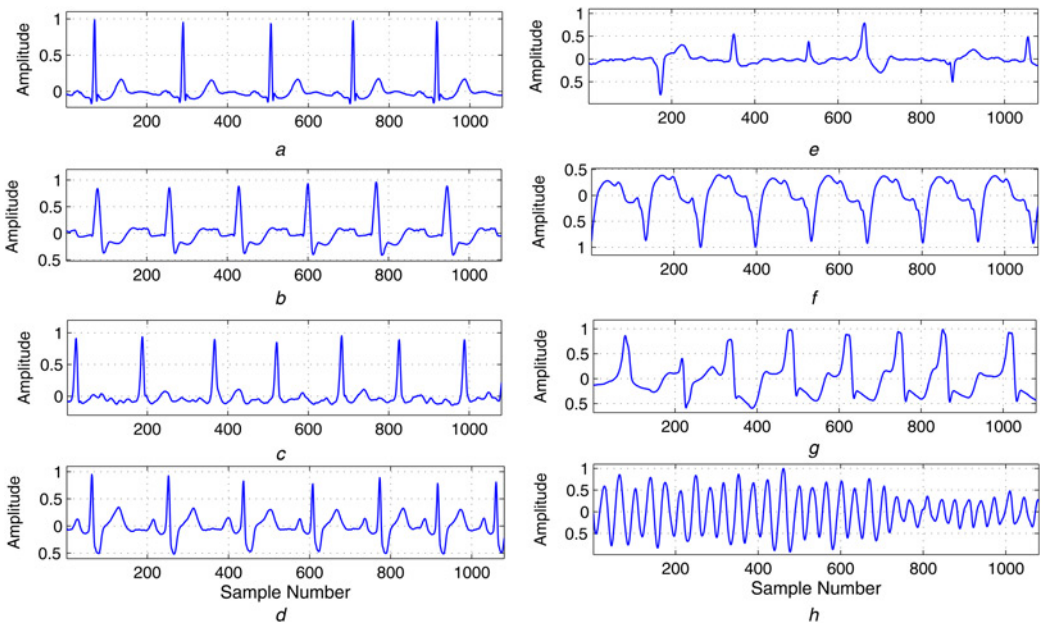

Fig. 1 *Illustrates the different ECG morphological patterns*
a–e Represents non-VTVF episodes taken from MIT-BIH arrhythmia database records 103, 109, 201, 212, 210, respectively
f–h Represents VT and VF episodes taken from CU VT database, respectively

(iv) Performance of the existing detection methods is not rigorously studied under different types of ECG noise sources and different PQRST morphological patterns.

In this Letter, we present an efficient and effective automated method for detection of VF and VT episodes under both noise and noise-free environments. The proposed method consists of four major stages: (i) discrete cosine transform (DCT)-based noise suppression; (ii) addition of bipolar sequence; (iii) ZCR estimation-based VTVF detection; and (iv) peak-to-peak interval (PPI) feature-based VT/VF discrimination. The proposed method is evaluated using 18,000 VTVF and non-VTVF episodes taken from six PhysioNet databases. Results show the promising results in identifying VTVF from non-VTVF episodes, and discriminating VT from VF episodes under both clean and noisy ECG signals corrupted with baseline wanders, PLI, MA, and other high-frequency noises.

The rest of this paper is organised as follows. Section 2 briefly describes the characteristics of the VT/VF events. Section 3 presents the proposed VT/VF detection method. In Section 4, the performance of the proposed method is evaluated using different types of ECG arrhythmias and various kinds of noise. Finally, conclusions are drawn in Section 5.

2. Life threatening arrhythmias: The VT and VF events are the most life threatening ventricular arrhythmias [3]. The VT is a very fast heart rhythm that begins in the ventricles. The characteristics of VT are [25] wide QRS complexes; heart rate more than 100 bpm (usually vary between 120 and 250 bpm); at least three heartbeats in a row although there may be some beat-to-beat variation; and the QRS axis is usually constant. The VT episodes can be classified as sustained (>30 s) or non-sustained VT (<30 s) and monomorphic or polymorphic. The VF is the most important shockable cardiac arrest rhythm. The characteristics of VF episodes are chaotic deflections of varying amplitude; no identifiable P/T waves and QRS complexes; rate varying between 250 and 500 bpm; and amplitude decreases with duration (coarse VF –> fine VF). The recent development and increased application of AEDs have prescribed very strong requirements towards detection of VF and fast VT (>180 bpm) episodes from the surface ECG signal.

From different kinds of ECG beats including the normal, left bundle branch block, right bundle branch block, atrial premature (AP), aberrated atrial and junctional premature beats, premature ventricular contraction, fusion of ventricular and normal, atrial and junctional escape beats, paced beat, fusion of paced and normal beats, atrial flutter, atrial fibrillation and blocked AP beat, it is noted that the most of the ECG arrhythmias are having the short and long PR and TP pause segments within cardiac cycles expect for the VT and VF episodes. Figs. 1*a–h* illustrate the characteristics of different types of ECG arrhythmias and VTVF episodes.

In this work, we exploit the long and short pause intervals for detecting the VT/VF events by adding bipolar sequence with alternating positive and negative polarities of amplitudes to an ECG signal. Figs. 2*a* and *b* illustrate the distributions of the ZCR values estimated for the different ECG arrhythmias before and after adding the bipolar sequence $w[n]$ to the ECG signals, respectively. From the ZCR distribution as shown in Fig. 2*a*, it is noted that the noise-free ECG signals have the lesser ZCR values that are not separable whereas Fig. 2*b* shows that the VTVF episodes are having the much lesser ZCR values than that of the other arrhythmia episodes that are separable after adding the bipolar sequence to the ECG signal. This is the basis for the proposed method of discriminating the VTVF episodes from non-VTVF episodes.

3. Proposed VT/VF detection method: In this work, we present an efficient and robust automated method for accurately detecting the VT/VF episodes under noise and noise free conditions. The proposed method consists of four major stages: (i) DCT-based filtering method for simultaneously removal of BW, PLI noises and smoothing out high-frequency noises; (ii) addition of bipolar sequence; (iii) ZCR estimation for discriminating VTVF episodes from non-VTVF episodes; and (iv) PPI feature-based VT/VF discrimination.

3.1. DCT-based noise suppression: The detection performance highly degraded under ECG signals corrupted with BW, PLI, and MA noises. Therefore, many signal processing techniques such as digital filters, adaptive filter, WT, and EMD are implemented to

doi: 10.1049/htl.2016.0010

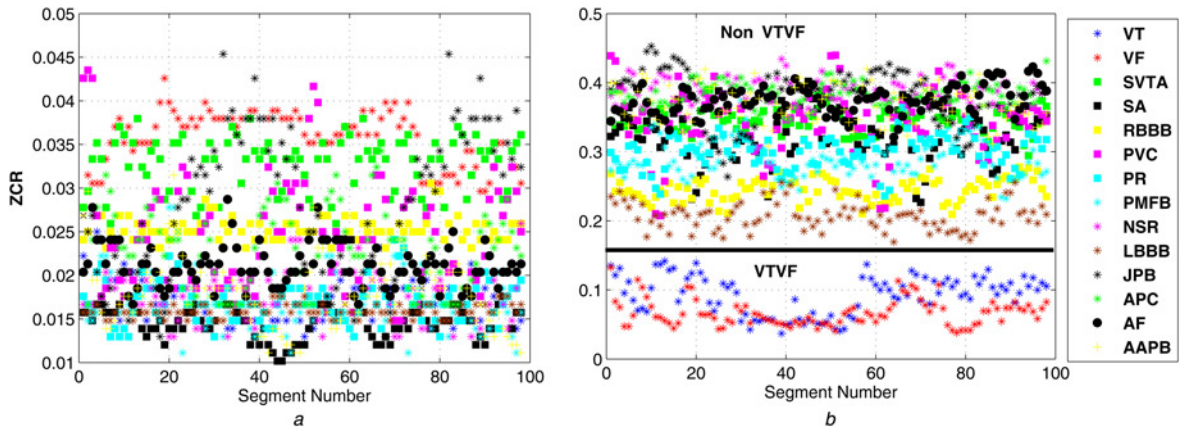

Fig. 2 *Illustrates the distribution of ZCR values estimated for different arrhythmias*
a Before adding the bipolar sequence
b After adding the bipolar sequence. The ZCR for the VTVF episodes is less than 0.15

remove ECG noises. Most methods use a high-pass filter (HPF) with cut-off frequency of 1 Hz to remove the baseline wanders and the Butterworth filter with a cut-off frequency of 30 Hz to remove PLI and muscle noises. It is difficult to design an HPF filter response with sharp attenuation to effectively remove baseline wanders with frequency less than 1 Hz without reducing the magnitude of the VT and VF signals with frequency range of 2–10 Hz. The DWT has spectral leakage problem. A selection of intrinsic mode functions is difficult under noise conditions. Since the baseline wander and PLI noise signals can be adequately captured using the elementary discrete sinusoids. Therefore, in this work, we present the DCT-based filtering approach to simultaneously remove baseline wander and PLI noises from the ECG signals. Further, we implement a hard thresholding rule with adaptive amplitude threshold to smooth out high frequency noises. As compared with the existing filtering approaches using the DWT and EMD, the DCT filtering approach is simple.

Let $x[n]$ be the input ECG sequence with length of N samples. The DCT of the $x[n]$ is computed as

$$c[k] = w[k]\sum_{n=1}^{N} x[n]\cos\left(\frac{\pi(2n-1)(k-1)}{2N}\right), \qquad (1)$$

where $w[k] = 1/\sqrt{N}\ k = 1, \sqrt{2/N}, \quad 2 \le k \le N$, $c[k]$ is the kth DCT coefficient [26]. In this work, we implement the DCT filtering approach for simultaneous removal of BW and PLI noises with the BW frequency range of 0–1 Hz and the grid power-line frequency range of 48–52 Hz. Fig. 3 illustrates the variation of the DCT coefficients (zoomed version up to 1000) for the noise-free ECG signal, the ECG plus BW and the ECG plus PLI signals. From the results, it can be observed that the ECG plus BW signal has the first few DCT coefficients having a very large amplitude as compared to noise-free ECG signal. Meanwhile, the ECG plus PLI signal has the middle DCT coefficients having the significant amplitude as compared to noise-free ECG signal. By discarding the those DCT coefficients,

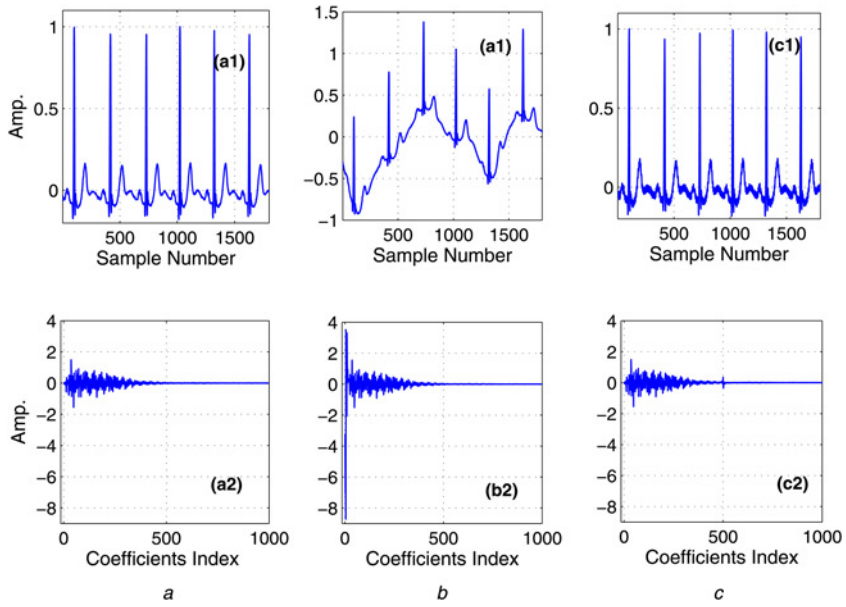

Fig. 3 *Illustrates the variations of DCT coefficients for the*
a Noise-free ECG signal
b ECG plus BW
c ECG plus PLI

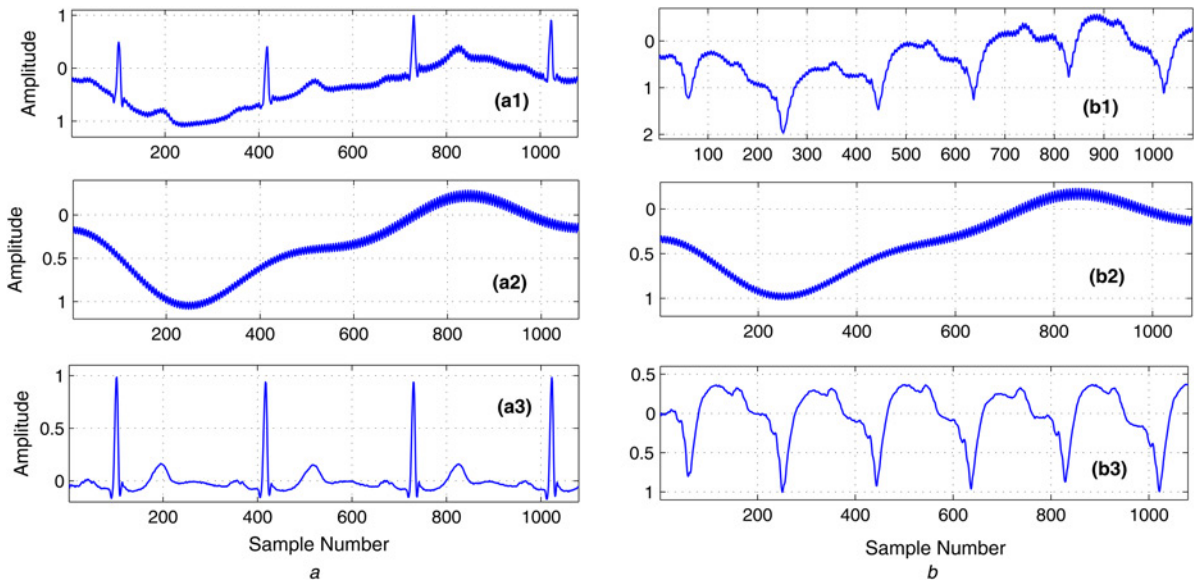

Fig. 4 *Illustrates the removal of BW and PLI noises from ECG signals using the DCT filtering approach: (a1) and (b1) are noisy normal ECG and VT signals; (a2) and (b2) are the extracted BW and PLI noises using DCT-based approach; (a3) and (b3) are the denoised ECG signals*

the BW and PLI noise signals can be removed from the ECG signals.

In this work, the DCT coefficient indexes for the predefined frequency ranges of the BW and PLI signals are computed as $k = (2 \times N \times f_k)/F_s$, where F_s is the sampling rate of a signal and f_k is the frequency of the kth DCT coefficient index. The removal of BW and PLI noise signals is implemented by zeroing the DCT coefficients of those frequency components. In practice, the ECG signal may be corrupted with an instrument noise. Therefore, we implement a hard thresholding rule with an adaptive threshold to smooth out high-frequency noise. The hard thresholding rule is defined as

$$\hat{c}[k] = \begin{cases} c[k], & |c[k]| > \eta_a \\ 0, & \text{otherwise}, \end{cases} \quad k = 1, 2, 3, \ldots, K, \tag{2}$$

where η_a is the amplitude threshold that is computed as the standard deviation of the DCT coefficient vector $\boldsymbol{c}$, and $\hat{\boldsymbol{c}}$ is the thresholded DCT coefficient vector. Then, the reconstructed signal is obtained by taking the inverse DCT of the thresholded coefficients. Fig. 4 illustrates the effectiveness of the DCT-based filtering approach for suppression of BW, PLI, and HF noises. From the filtering results, it is noted that the BW and PLI noises are significantly removed from the noisy ECG signals. In this work, the DCT-based smoothing is implemented to increase the robustness in estimating the zero-crossing rates as well as to obtain robust temporal features.

3.2. VTVF/non-VTVF discrimination using ZCR measurement: In this work, we exploit a total number of zero-crossings in the pause intervals between the local waves (including, $P_{end} - Q_{on}$, $S_{end} - T_{on}$, and $T_{end} - P_{on}$ of the filtered ECG signal $s[n]$ is used for discriminating the VTVF episodes from the non-VTVF episodes. In order to reduce the effect of low-amplitude fluctuating components, we add bipolar sequence $w[n]$ of amplitudes with alternating polarities to the processed ECG signal. The feature signal $z[n]$ is computed as the additive mixture of the filtered ECG signal $s[n]$ and the bipolar sequence $w[n]$ with length of N samples that has higher zero-crossings of $N-1$. The feature signal $z[n]$ is obtained as

$$z[n] = s[n] + w[n]. \tag{3}$$

For the feature signal $z[n]$, the ZCR is computed as

$$\text{ZCR} = \frac{1}{N}\sum_{n=0}^{N} |\text{sgn}(z[n]) - \text{sgn}(z[n-1])|, \tag{4}$$

where N denotes the number of samples [27]. In this work, the ZCR value obtained for a 3 s ECG signal is used to discriminate the VTVF episodes from the non-VTVF episodes. For a total number of 1170 VTVF and non-VTVF segments with a segment duration of 3 s, the global ZCR values estimated for different kinds of the ECG arrhythmias are shown in Figs. 5*a* and *b* before and after adding the bipolar sequences to the filtered ECG signals. From the ZCR distribution as shown in Fig. 5*a*, it is observed that the noise-free ECG segments have the zero-crossing rates that are not separable. After adding the bipolar noise sequence to the noise-free ECG segments, the distribution of global ZCR values as shown in Fig. 5*b* show that a ZCR value of 0.17 is the best ZCR threshold for discriminating the VTVF episodes from the non-VTVF episodes. From the ZCR distribution as shown in Fig. 2*b* obtained for 98 segments of all types of arrhythmias, it is noted that the global ZCR value is capable of discriminating the VTVF episodes from the other ECG arrhythmias.

In this work, classification of VTVF and non-VTVF episodes is performed by comparing the measured global ZCR value for the 3 s VTVF and non-VTVF episodes with a predefined ZCR threshold value of 0.17. The VTVF detection rule is defined as

$$\text{Output} = \begin{cases} \text{VTVF episode}, & \text{ZCR} < \text{ZCR}_{th} \\ \text{non-VTVF episode}, & \text{otherwise}. \end{cases} \tag{5}$$

3.3. PPI-based VT/VF discrimination: In this stage, the detected VTVF episodes are processed for discriminating VF from VT events. In most scenarios, it is noted that the heart rates are different for the VT (100–250 bpm) and VF (250–500 bpm) segments and shapes of the positive and negative half cycles are different. In this work, the temporal features including mean estimates of the positive PPI (PPPI) and negative PPI (NPPI) are extracted from the filtered ECG signal. The steps involving in finding the above features include: (i) find positive and negative zero-crossings; (ii) find the minimum between positive and negative zero-crossings and the maximum between negative and

doi: 10.1049/htl.2016.0010

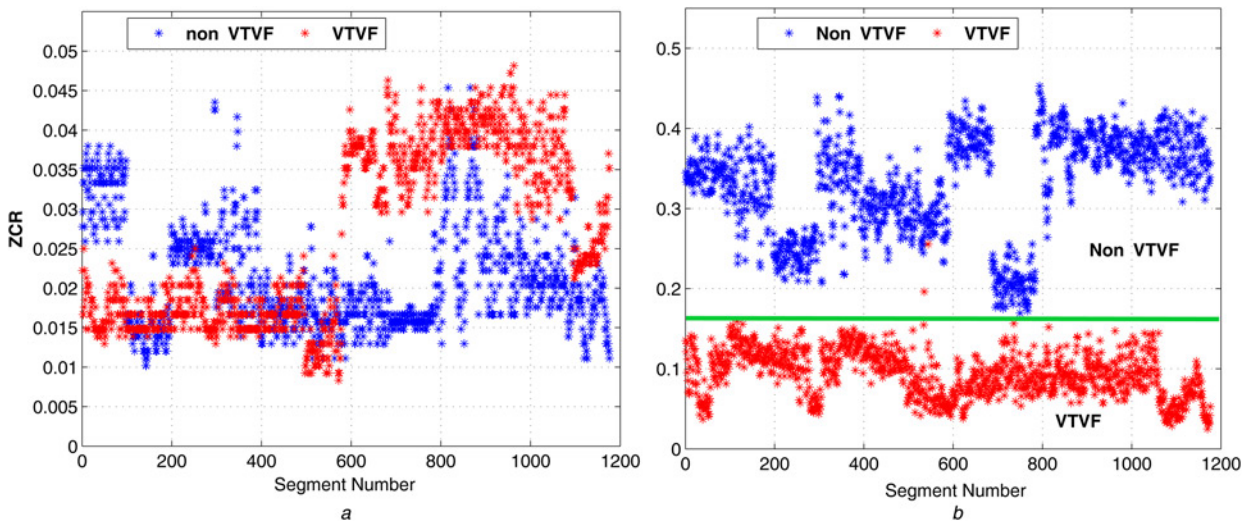

Fig. 5 *Illustrates the distribution of ZCR values estimated for VTVF and non-VTVF episodes*
a Before adding the bipolar sequence
b After adding the bipolar sequence. It shows that the capability of ZCR value in discriminating the VTVF episodes from the non-VTVF episodes

positive zero-crossings; (iii) find the mean of the PPP intervals as well as NPP intervals to obtain the representative features including the PPPI and NPPI. Fig. 6 illustrates the representation of temporal features for the VT and VF segments. The effectiveness of the those features is illustrated in Figs. 7*a* and *b* using 500 VT/VF segments with segment duration of 3 s. Results show that the distributions of the mean estimates of the PPPI and NPPI features (in ms) estimated for the VT and VF segments. It is observed that the mean estimates of the PPPI and NPPI features are capable of separating the VT from VF segments. In this work, the 3 s VTVF segments are classified as VT and VF events by comparing the estimated mean PPPI and NPPI values with a predefined interval threshold of 250 ms as shown in Figs. 7*a* and *b*. The VT/VF discrimination rule is defined as

$$\text{Output} = \begin{cases} \text{VF episode}, & \text{PPPI} < T_{\text{th}} \text{ and NPPI} < \eta_I \\ \text{VT episode}, & \text{otherwise.} \end{cases} \quad (6)$$

4. Results and discussion: In this section, we evaluate the effectiveness of the proposed method using 18,000 VTVF and non-VTVF episodes taken from 6 Physionet databases [28]: MIT-BIH arrhythmia database (MITADB), the Creighton university VT database (CUVTDB), the MIT-BIH malignant VT database (MITMVTDB), the normal sinus rhythm database (NSRDB), noise stress test database (NSTDB), the ST change database (STCDB). The duration of episode is 3 s. The test ECG databases include different kinds of PQRST morphological patterns (such as, sharp and tall P and T waves, negative QRS complex, small QRS complex, and wider QRS complex), regular and irregular rhythms, short and long pauses and different kinds of noise such as baseline wanders, powerline interference, and muscle artefacts. Our test databases include the following types of non-VT–VF beats: normal beat; left bundle branch block; right bundle branch block; atrial premature complex (APC); aberrated atrial premature; nodal (junctional) premature; premature ventricular contraction; fusion of ventricular and normal beats; fusion of paced and normal beats; blocked APC; and the ventricular tachycardia; and ventricular fibrillation episodes.

The performance of the VTVF detection method is evaluated in terms of three benchmark parameters: the sensitivity (Se), specificity (Sp), overall accuracy (OA) that are computed as

$$\text{Se}\ (\%) = \frac{\text{TN}}{\text{TN} + \text{FP}} \times 100 \quad (7)$$

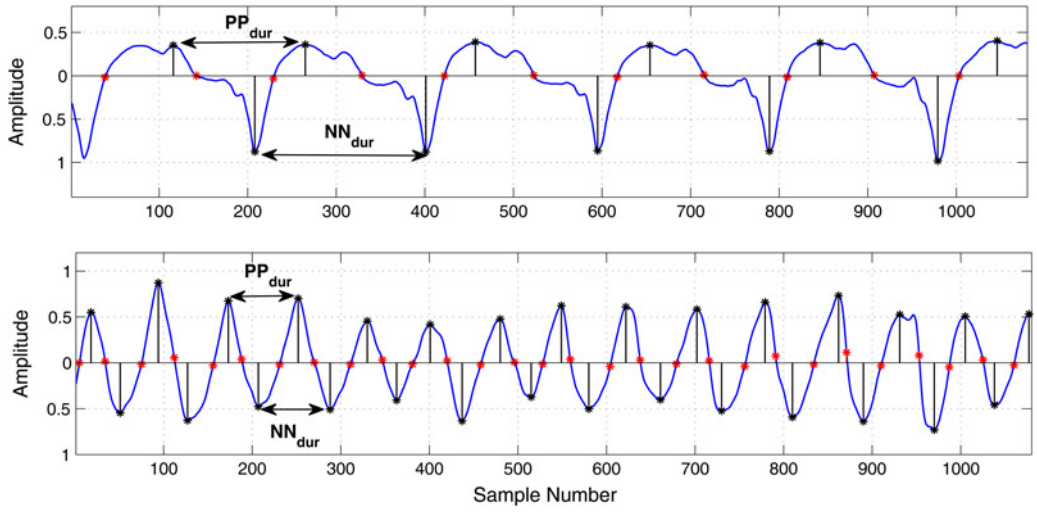

Fig. 6 *Illustrates the measurement of temporal features such as PPPI and NPPI for discriminating the VT episode from the VF episode*

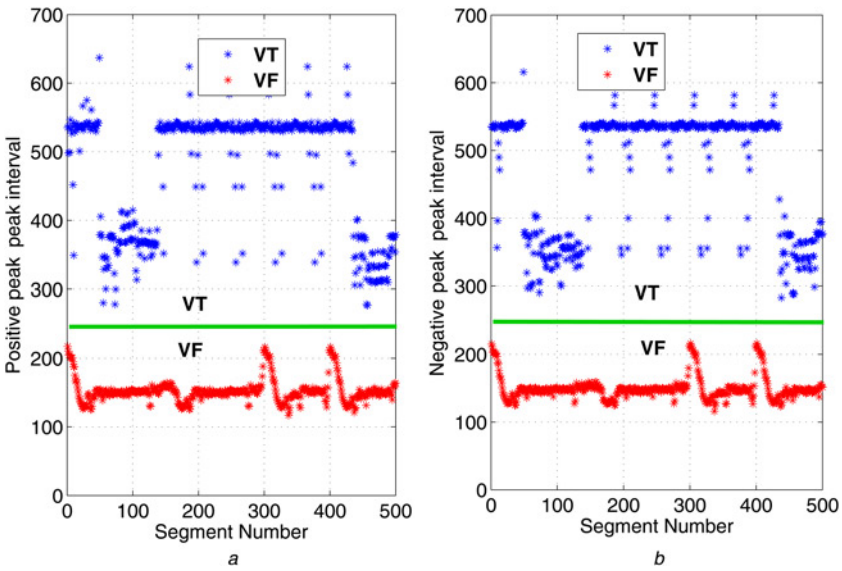

Fig. 7 *Illustrates the distributions of the temporal features extracted from VT and VF episodes*
a PPPI features
b NPPI features

Table 1 Performance of the method for different ZCR thresholds

ZCR_{th}	NS	FP	FN	TP	TN	Se, %	Sp, %	OA, %
0.15	1200	78	0	600	522	87	100	93.5
0.16	1200	35	0	600	565	94	100	97.08
0.17	1200	3	0	600	597	99.5	100	99.75

NS: number of segments; VTVF: 600 and non-VTVF: 600

$$\text{Sp}\ (\%) = \frac{\text{TP}}{\text{TP} + \text{FN}} \times 100 \tag{8}$$

$$\text{OA}\ (\%) = \frac{\text{TP} + \text{TN}}{\text{TP} + \text{TN} + \text{FP} + \text{FN}} \times 100 \tag{9}$$

where true negative (TN) denotes VTVF episode being classified as VTVF and false positive (FP) denotes VTVF episode being miss-classified as non-VTVF episode, true positive (TP) denotes non-VTVF episode being classified as non-VTVF episode and false negative (FN) denotes non-VTVF episode being miss-classified as VTVF episode.

In the first experiment, we study a selection of optimal ZCR threshold using the 1200 VTVF and non-VTVF segments. Table 1 summarises the detection results for the ZCR thresholds of 0.15, 0.16, and 0.17 that are obtained from the ZCR distribution as shown in Figs. 2*b* and 5*b*. From the results, it is noted that the method has better detection results for ZCR threshold of 0.17. The reference ZCR threshold line is shown in Figs. 2*b* and 5*b*. In this work, a ZCR threshold of 0.17 is chosen for further performance comparison. Table 2 summarises the detection results of the proposed method for the VTVF and non-VTVF episodes taken from six standard ECG databases. From the results, it is noted that the method has a Se of 99.61% for a total of 2058 VTVF episodes taken from the CUDB, VFDB, and MITDB. The method has an average Se of 99.61%, Sp of 99.96%, and OA of 99.92% for a total of 18,000 episodes including the 15,942 non-VTVF episodes and 2058 VTVF episodes. From the results, it is noted that the method fails to detect the short-duration VTVF episodes which are less than 2 s that are mixed with the non-VTVF events in the 3 s ECG signal.

In the second experiment, we study the robustness of the method using the 600 VTVF segments and 600 non-VTVF segments for the ECG noises including BW, MA and PLI and additive white Gaussian noise (AWGN) with signal-to-noise ratios (SNRs) ranging from 30 to 10 dB. Table 3 summarises the detection results of the proposed method. It is noted that the method can achieve a Se of 99.33%, Sp of 100%, and OA of 99.67% for VTVF and non-VTVF episodes with SNR of 10 dB. Table 4 summarises the performance of the method in discriminating the VT from VF episodes for a total of 2000 VT/VF episodes taken from the Creighton university and MIT-BIH malignant VT databases. The method achieves a Se of 100%, Sp of 99.70%, and OA of 99.85%.

Based upon comparison results as shown in Table 5, it is noted that the proposed method outperforms the other detection methods based on the sets of features extracted in time-domain, frequency-domain and decomposed signals and the machine learning approaches. Furthermore, it is noted that the proposed method employs a simple DCT filtering approach and single ZCR feature

Table 2 Results of the non-VTVF/VTVF episode discrimination

Database	NS	FP	FN	TP	TN	Se, %	Sp, %	OA, %
MITDB	13,000	4	0	12,942	54	93.10	100	99.97
CUDB and VFDB	2000	4	0	0	1996	99.8	–	99.8
NSRDB	1000	0	0	1000	0	–	100	100
STDB	1000	0	0	1000	0	–	100	100
NSTDB	1000	0	6	994	0	–	99.40	99.40
overall	18,000	8	6	15,936	2050	99.61	99.96	99.92

doi: 10.1049/htl.2016.0010

Table 3 Performance of the method under BW, MA, and PLI noises and different SNRs

Noise type	NS	FP	FN	TP	TN	Se, %	Sp, %	OA, %
PLI+BW	1200	3	4	596	597	99.5	99.33	99.42
MA	1200	2	0	600	598	99.67	100	99.83
30 dB	1200	3	0	600	597	99.5	100	99.75
20 dB	1200	3	0	600	597	99.5	100	99.75
10 dB	1200	4	0	600	596	99.33	100	99.67

Table 4 VT/VF classification performance of the proposed method

Event	NS	FP	FN	TP	TN	Se, %	Sp, %	OA, %
VT	1000	0	–	–	1000	100	–	100
VF	1000	3	–	997	–	–	100	99.70
overall	2000	0	3	997	1000	100	99.70	99.85

in detecting the VTVF episodes and two temporal features for discriminating the VF episodes from the VT episodes. The proposed method is implemented using MATLAB with Intel i3 Processor, 1.90 GHz, 4 GB RAM. The computational time for the most widely used signal processing techniques such as WT, variational mode decomposition, EMD, and DCT. Based on the computational

Table 5 Performance comparison of detection methods

Ref.	Techniques	Performance	Database
[2]	Baseline wander and PLI removal, SVM, 14 features, GA	AC = 96.3%, Se = 98.4%, Sp = 98.0%	MITDB, CUDB, AHADB
[3]	Mean subtraction, moving average filter, HPF, LPF, SVM, 13 features, FS-filtering	Shockable: Se = 95%, Sp = 99.0%,VFib: Se = 92%, Sp = 97%	CUDB, MITDB
[5]	Mean subtraction, moving average filter, HPF, LPF, SVM, 11 features	VF against non-VF: AUC = 0.96%, Se = 81%, Sp = 85%. shockable against non-shockable: AUC = 0.99%, Se = 96%, Sp = 99%	MITDB, CUDB, VFDB
[6]	Bandpass filter, CWT, scalogram, two features, LDA	Classification: VF as VF = 75% and as VT–VF = 25%, VT–VF as VT–VF = 75% and as VF = 25%, VT as VT = 75% and as VT–VF = 25%	MITDB
[7]	Haar wavelet, 14 features, NFN with WFM functions	AC = 92%, Se = 93%	CUDB
[8]	Bandpass filter and time-delay method	Se = 79%, Sp = 97.8%	MITDB
[29]	Wavelet, DCT, PCA, PNN	Se = 98.69%, Sp = 99.91%, AC = 99.52%	MITDB
our method	DCT-based noise removal, ZCR and PPI features	VTVF/non-VTVF Detection: Se = 99.61%, Sp = 100%, OA = 99.61%. VT/VF detection: Se = 100%, Sp = 99.70%, OA = 99.85%	MITDB, CUDB, VFDB

Table 6 Computational time of the signal processing techniques

Signal processing method	Coding, ms
WT	10.2
variational mode decomposition	305.5
EMD	35871.9
DCT	0.78125

results summarised in Table 6, the proposed method has an encoding time of 0.781 ms that is much lesser than the other methods. In future directions, we extend a further in-depth study on reducing computational load by implementing the proposed method on real-time signal processor hardware platforms.

5. Conclusion: In this Letter, an efficient and robust method for automatically detecting VTVF episodes and discriminating the VT episodes from the VF episodes using bipolar sequence with alternating polarities of amplitudes and temporal features such as ZCR, positive and negative peak to peak intervals. In this work, we present DCT-based filtering approach for simultaneously removal of BW and PLI and high-frequency noises. The proposed method is evaluated using a total of 18,000 VTVF and non-VTVF episodes taken from the 6 standard ECG databases such as MITADB, CUVTDB, MITMVADB, NSRDB, NSTDB, and STCDB. The method achieves an overall Se of 99.61%, Sp of 99.96%, and OA of 99.92% in discriminating the VTVF episodes from the non-VTVF episodes. The method achieves an overall Se of 100%, Sp of 99.70%, and OA of 99.85% in discriminating the VF episodes from the VT episodes. Evaluation results show that the proposed method can achieve significantly better detection rates as compared with the existing methods.

6. Funding and declaration of interests: Conflict of interest declared: none.

7 References

[1] Chong J.W., Esa N., McManus D.D., *ET AL.*: 'Arrhythmia discrimination using a smart phone', *IEEE Trans. Biomed. Eng.*, 2015, **19**, (3), pp. 1–4

[2] Qiao L., Rajagopalan C., Clifford G.D.: 'Ventricular fibrillation and tachycardia classification using a machine learning approach', *IEEE Trans. Biomed. Eng.*, 2014, **61**, (6), pp. 1607–1613

[3] Alonso-Atienza F., Morgado E., Fernández-Martínez L., *ET AL.*: 'Detection of life-threatening arrhythmias using feature selection and support vector machines', *IEEE Trans. Biomed. Eng.*, 2014, **61**, (3), pp. 832–840

[4] Chen S., Thakor N.V., Mower M.M.: 'Ventricular fibrillation detection by a regression test on the autocorrelation function', *Med. Biol. Eng. Comput.*, 1987, **25**, pp. 241–249

[5] Alonso-Atienza F., Morgado E., Fernández-Martínez L., *ET AL.*: 'Combination of ECG parameters with support vector machines for the detection of life-threatening arrhythmias'. Proc. Comput. Cardiol., September 2012, vol. **39**, pp. 385–388

[6] Balasundaram K., Masse S., Nair K., *ET AL.*: 'Wavelet-based features for characterizing ventricular arrhythmias in optimizing treatment options'. Proc. IEEE EMBS, 2011, pp. 969–972

[7] Zhen-Xing Z., Tian X.W., Lim J.S.: 'Real-time algorithm for a mobile cardiac monitoring system to detect life-threatening arrhythmias'. Proc. Int. Conf. Computer and Automation Engineering, February 2010, vol. **4**, pp. 232–236

[8] Amann A., Tratnig R., Unterkofler K.: 'Detecting ventricular fibrillation by time-delay methods', *IEEE Trans. Biomed. Eng.*, 2007, **54**, (1), pp. 174–177

[9] Arafat M., Chowdhury A., Hasan M.: 'A simple time domain algorithm for the detection of ventricular fibrillation in electrocardiogram', *Signal, Image, Video Process.*, 2011, **5**, pp. 1–10

[10] Thakor N.V., Zhu Y.S., Pan K.Y.: 'Ventricular tachycardia and fibrillation detection by a sequential hypothesis testing algorithm', *IEEE Trans. Biomed. Eng.*, 1990, **37**, (9), pp. 837–43

[11] Anas E., Lee S., Hasan M.: 'Sequential algorithm for life threatening cardiac pathologies detection based on mean signal strength and emd functions', *BioMed. Eng. OnLine*, 2010, **9**, (1), pp. 43–64
[12] Zhang X.-S., Zhu Y.-S., Thakor N.V., *ET AL.*: 'Detecting ventricular tachycardia and fibrillation by complexity measure', *IEEE Trans. Biomed. Eng.*, 1999, **46**, (5), pp. 548–55
[13] Li H., Han W., Hu C., *ET AL.*: 'Detecting ventricular fibrillation by fast algorithm of dynamic sample entropy'. Proc. IEEE Robot. Biomimet., 2009, pp. 1105–1110
[14] Clayton R.H., Murray A., Campbell R.W.: 'Recognition of ventricular fibrillation using neural networks', *Med. Biolog. Eng. Comput.*, 1994, **32**, (2), pp. 217–220
[15] Clayton R.H., Murray A., Campbell R.W.F.: 'Comparison of four techniques for recognition of ventricular fibrillation from the surface ECG', *Med. Biol. Eng. Comput.*, 1993, **31**, pp. 111–117
[16] Jekova I., Mitev P.: 'Detection of ventricular fibrillation and tachycardia from the surface ECG by a set of parameters acquired from four methods', *Physiol. Meas.*, 2002, **23**, pp. 629–634
[17] Jekova I., Dushanova J., Popivanov D.: 'Method for ventricular fibrillation detection in the external electrocardiogram using nonlinear prediction', *Physiol. Meas.*, 2002, **23**, pp. 337–345
[18] Krasteva V., Jekova I.: 'Assessment of ECG frequency and morphology parameters for automatic classification of life-threatening cardiac arrhythmias', *Physiol. Meas.*, 2005, **26**, (5), pp. 707–723
[19] Wang Y., Zhu Y.-S., Thakor N.V., *ET AL.*: 'A short-time multifractal approach for arrhythmia detection based on fuzzy neural network', *IEEE Trans. Biomed. Eng.*, 2001, **48**, (9), pp. 989–995
[20] Khadra L., Fahoum A.S.A., Nashash H.A.: 'Detection of life-threatening cardiac arrhythmias using the wavelet transformation', *Med. Biol. Eng. Comput.*, 1997, **35**, pp. 625–632
[21] Dorsett T.J., Guilak F., Taylor A.L.: 'A real-time ventricular arrhythmia detection system based on the KL transform and sequential-hypothesis testing'. Proc. IEEE EMBS, September 1997, vol. 2, pp. 1007–1008
[22] Arrobo G.E., Perumalla C.A., Hanke S.B., *ET AL.*: 'An innovative wireless cardiac rhythm management (iCRM) system'. Wireless Telecommunications Symp., 2014
[23] Lim J.S.: 'Finding features for real-time premature ventricular contraction detection using a fuzzy neural network system', *IEEE Trans. Neural Netw.*, 2009, **20**, (3), pp. 522–527
[24] Prabhakararao E., Sabarimalai Manikandan M.: 'Detection of life-threatening arrhythmias using random noise and zerocrossing information'. Proc. IEEE Int. Conf. Wireless Communications, Signal Processing and Networking – WiSPNET, March 2016
[25] Huszar J.R.: 'Basic dysrhythmias, interpretation and management' (Mosby Co., St. Louis, 1988)
[26] Sabarimalai Manikandan M., Samantaray S.R., Kamwa I.: 'Simultaneous denoising and compression of power system disturbances using sparse representation on over complete hybrid dictionaries', *IET Gener. Transm. Distrib.*, 2015, **9**, (11), pp. 1077–1088
[27] Kathirvel P., Sabarimalai Manikandan M., Senthilkumar S., *ET AL.*: 'Noise robust zerocrossing rate computation for audio signal classification'. Proc. Third Int. Conf. Trendz in Information Sciences and Computing (TISC), 2011, pp. 65–69
[28] http://www.physionet.org/physiobank/database
[29] Martis R.J., Rajendra Acharya U., Lim C.M., *ET AL.*: 'Characterization of ECG beats from cardiac arrhythmia using discrete cosine transform in PCA framework', *Knowl. Based Syst.*, 2013, **45**, pp. 76–82

doi: 10.1049/htl.2016.0010